This article was downloaded by:
On: *28 January 2011*
Access details: *Access Details: Free Access*
Publisher *Taylor & Francis*
Informa Ltd Registered in England and Wales Registered Number: 1072954 Registered office: Mortimer House, 37-41 Mortimer Street, London W1T 3JH, UK

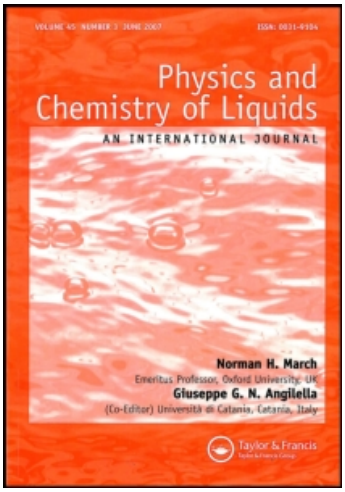

Physics and Chemistry of Liquids
Publication details, including instructions for authors and subscription information:
http://www.informaworld.com/smpp/title~content=t713646857

Statistical Mechanical Theory of Rod-Like Molecular Fluids with Kihara-Type Interactions. I. Molecular Distribution Functions

M. Lombardero[ab]; S. Lago[abc]
[a] Instituto de Química Física Rocasolano del CSIC, Madrid, Spain [b] Departamento de Química Física. Facultad de Ciencias Químicas, Universidad Complutense, Madrid, Spain [c] Rhur Universität Bochum, Inst. Thermo-und Fluiddynamik, Bochum, FRG

To cite this Article Lombardero, M. and Lago, S.(1981) 'Statistical Mechanical Theory of Rod-Like Molecular Fluids with Kihara-Type Interactions. I. Molecular Distribution Functions', Physics and Chemistry of Liquids, 11: 2, 141 — 155
To link to this Article: DOI: 10.1080/00319108108079106
URL: http://dx.doi.org/10.1080/00319108108079106

PLEASE SCROLL DOWN FOR ARTICLE

Full terms and conditions of use: http://www.informaworld.com/terms-and-conditions-of-access.pdf

This article may be used for research, teaching and private study purposes. Any substantial or systematic reproduction, re-distribution, re-selling, loan or sub-licensing, systematic supply or distribution in any form to anyone is expressly forbidden.

The publisher does not give any warranty express or implied or make any representation that the contents will be complete or accurate or up to date. The accuracy of any instructions, formulae and drug doses should be independently verified with primary sources. The publisher shall not be liable for any loss, actions, claims, proceedings, demand or costs or damages whatsoever or howsoever caused arising directly or indirectly in connection with or arising out of the use of this material.

Phys. Chem. Liq., 1981, Vol. 11, pp. 141–156
0031-9104/81/1102-0141$06.50/0
© 1981 Gordon and Breach Science Publishers, Inc.
Printed in the U.S.A.

Statistical Mechanical Theory of Rod-Like Molecular Fluids with Kihara-Type Interactions

I. Molecular Distribution Functions

M. LOMBARDERO and S. LAGO†

Instituto de Química Física Rocasolano del CSIC. Serrano, 119. Madrid–6, Spain.

and

Departamento de Química Física. Facultad de Ciencias Químicas. Universidad Complutense. Madrid–3, Spain.

(Received February 23, 1981)

Downloaded At: 08:51 28 January 2011

A simplified integral equation for the pair distribution function of linear molecules interacting via a potential depending only on the shortest distance between molecular cores, is written down. The theory is developed starting from the Ornstein–Zernike equation and the Percus–Yevick closure relation, both for non-spherical particles. Two basic assumptions are made. Firstly the molecular pair distribution function is supposed to depend explicitly on the shortest distance but not on molecular orientations; secondly the direct correlation function inside the integral in the Ornstein–Zernike equation is approximated by some average value conveniently defined.

The new integral equation is numerically solved for CO_2 and N_2 assuming a Kihara potential. The main features of the distribution function, particularly its behaviour with temperature and density, are also investigated. The results obtained seem to agree well with a very probable structural model for liquid CO_2 and a reasonable model for N_2.

I INTRODUCTION

Up until the end of the past decade, research in Classical Statistical Mechanics on fluids in equilibrium has been practically restricted to "simple liquids," where interactions can be adequately modelled by spherically symmetrical potentials.

† Present address: Rhur Universität Bochum, Inst. Thermo- und Fluiddynamik, 4630 Bochum 1. FRG.

The advances at the theoretical level as well as the results achieved by model simulation methods (Monte Carlo and Molecular Dynamics), supported by a wealth of experimental information, have enabled us to make substantial progress in the knowledge of these systems.[1]

It is only in the last few years when increasing interest has been centered on polyatomic fluids interacting with non-central forces; nevertheless, significant advances have been already made in developing theories for such systems.

For non-polar molecular liquids made up of rigid non-spherical particles, two different types of potential models have been proved to be useful in the description of their intermolecular forces: "atom-atom" or interaction site model (ISM) potentials[2] and those of Kihara core type.[3] The first one has been widely used to interpret the local structure of dense liquids both from the point of view of Statistical Mechanics[4] and model simulation.[5] On the other hand, first-order perturbation theories have been recently formulated by Ladanyi and Chandler[3] for ISM potentials and by Boublík[6] for Kihara systems. Finally, under certain approximations, the Percus-Yevick (PY) integral equation, generalized for angle-dependent non-spherical potentials, has been considered by Chen and Steele[7] and by Ben-Naim[8] to calculate the pair correlation function of liquid water with a water-like interaction potential.

In this paper, we propose a different approximation based also on PY equation for non-spherical molecules. Our approximation have been particularly thought out for linear molecules which can be modelled by a hard core linear segment with interactions depending only on the shortest distance, ρ, between cores. The basic idea of this theory is the assumption that the pair distribution function, like the intermolecular potentials, depends only on ρ. With this assumption and some supplementary but important approximations we write down in the next section an integral equation for the pair distribution function, whose main feature is its relative simplicity. It shows a similar structure of the primitive PY's for spherical molecules, so that one may apply some of the same numerical methods of solution developed for the last one. By using the Broyles's method[9] (whose adaptation to our case is considered in Section 3), the equation is solved for nitrogen and carbon dioxide in the same Section 3. Numerical calculations have been carried out with the Kihara potential:

$$u(\rho) = 4\varepsilon\left(\left(\frac{\sigma}{\rho}\right)^{12} - \left(\frac{\sigma}{\rho}\right)^{6}\right) \tag{1}$$

where ε is the potential well depth and σ is the shortest distance defined as $u(\sigma) = 0$.

In Section 4, the calculated results are used to analyze the pair distribution function and its dependence on density and temperature. Section 5 is de-

Downloaded At: 08:51 28 January 2011

voted to a discussion of possible liquid structures; conclusions are presented in Section 6.

II INTEGRAL EQUATION FOR THE PAIR DISTRIBUTION FUNCTION

Our system consists of a one-component fluid containing N non-spherical molecules in a volume V at temperature T. It is assumed that the molecules can be well represented by hard linear segments interacting via a potential $u(\rho)$ which depends only on the shortest distance, ρ, between two segments. If L stands for the segment length, then the volume V_c, surface area S_c, and mean curvature R_c of the core are $V_c = S_c = 0$, $R_c = \pi L$.

On the other hand, for molecules with angle-dependent intermolecular potential, the generalized Ornstein–Zernike (OZ) equation[10] is written as

$$h(\mathbf{q}_1, \mathbf{q}_2) = c(\mathbf{q}_1, \mathbf{q}_2) + \left(\frac{n}{8\pi^2}\right) \int_{\mathscr{R}} (\mathbf{q}_1, \mathbf{q}_3) c(\mathbf{q}_2, \mathbf{q}_3)\, \mathrm{d}\mathbf{q}_3 \tag{2}$$

where the notation is as follows. If $\mathbf{R}$ is the center of mass position vector and $\mathbf{\Omega}$ denotes the orientational angles (Euler angles), then $\mathbf{q}$ stands for the set of translational and rotational coordinates $\{\mathbf{R}, \mathbf{\Omega}\}$ and $\mathrm{d}\mathbf{q} = \mathrm{d}\mathbf{R} \cdot \mathrm{d}\mathbf{\Omega}$ is the volume element in the $\mathbf{q}$-hyperspace. The symbol $\mathscr{R}$ in the r.h.s. of Eq. (2) means the region in the $\mathbf{q}$-space over which the integral must be evaluated; $h(\mathbf{q}, \mathbf{q}')$, defined in terms of the pair distribution function $g(\mathbf{q}, \mathbf{q}')$ by

$$h(\mathbf{q}, \mathbf{q}') = g(\mathbf{q}, \mathbf{q}') - 1 \tag{3}$$

and $c(\mathbf{q}, \mathbf{q}')$ as defined by the OZ equation, are respectively the total and direct correlation functions. Finally, $n = N/V$ is the number density. The rotational coordinates are defined so that

$$\int \mathrm{d}\mathbf{\Omega} = 8\pi^2 \tag{4}$$

By inserting in Eq. (2) the Percus–Yevick approximation

$$c(\mathbf{q}, \mathbf{q}') = g(\mathbf{q}, \mathbf{q}')\left(1 - \exp\left(\frac{u(\mathbf{q}, \mathbf{q}')}{kT}\right)\right) \tag{5}$$

where k is the Boltzmann's constant and $u(\mathbf{q}, \mathbf{q}')$ the intermolecular potential, one obtains the Percus–Yevick equation in the generalized form

$$g(\mathbf{q}_1, \mathbf{q}_2) \exp\left(\frac{u(\mathbf{q}_1, \mathbf{q}_2)}{kT}\right) = 1 + \left(\frac{n}{8\pi^2}\right) \int (g(\mathbf{q}_1, \mathbf{q}_3) - 1) \times (1 - \exp(u(\mathbf{q}_2, \mathbf{q}_3)))g(\mathbf{q}_2, \mathbf{q}_3)\, \mathrm{d}\mathbf{q}_3 \tag{6}$$

In its exact form this equation is unmanageable. Being an integral equation to be solved in a five-dimensional (for linear molecules) or six-dimensional (for non-linear molecules) space, it cannot be handled even by the fastest

Downloaded At: 08:51 28 January 2011

and more powerful computers available today. For instance, it was estimated[8] that to evaluate $g(\mathbf{q}, \mathbf{q}')$ for only ten values for each of the six independent variables require 10^6 minutes of computational time, at least.

For molecules with a water-like interaction potential, Ben-Naim[8] has proposed an approximate theory for the pair correlation function $g(\mathbf{q}, \mathbf{q}')$. Basically, he assumes that the potential of the average forces can be split up into a direct and an indirect part, the last being a function only of the distance between the centers of mass of the corresponding molecules. Under this assumption it is possible to write Eq. (6) in a form ready for numerical integration. However, Ben-Naim's theory does not seem adequate for particles interacting with a Kihara type potential, as is our case.

We will assume first that the pair potential $w(\mathbf{q}, \mathbf{q}')$ of the average forces is only a function of the shortest distance, ρ, as is the case with the interaction potential, $u(\rho)$. Then, taking into account the relationship

$$g = \exp\left(-\frac{w}{kT}\right) \tag{7}$$

between the pair correlation function g and w, it follows that $g((g(\mathbf{q}, \mathbf{q}') \to g(\rho))$ and the total correlation function h (see Eq. (3)) depend only on ρ. This is also true for the direct correlation function c, if one assumes a closure relation of the Percus–Yevick type,

$$c(\rho) = g(\rho)\left(1 - \exp\left(\frac{u(\rho)}{kT}\right)\right) \tag{8}$$

Starting from Eq. (2) and using relation (8), we try now to write down an integral equation for $g(\rho)$. For correlation functions $h(\rho)$ and $c(\rho)$ Eq. (2) yields

$$h(\rho_{12}) = c(\rho_{12}) + \left(\frac{n}{8\pi^2}\right) \int h(\rho_{13})c(\rho_{23})\, \mathrm{d}\mathbf{q}_3 \tag{9}$$

However, this equation is almost as unmanageable as the initial one and therefore it requires some further simplification. The main source of trouble is that the distance ρ_{23}, and consequently $c(\rho_{23})$ too, appearing under the integral in Eq. (9), depends in a rather complicated way on ρ_{12} and ρ_{13} and also on the orientation $\mathbf{\Omega}_3$ of molecule 3. Keeping this in mind, we apply one of the simplest assumptions one can think of, that is, substituting the correlation function $c(\rho_{23})$ by its average value

$$\langle c \rangle = (\rho_{12} + \rho_{13} + L - m_1)^{-1} \int_{m1}^{\rho_{12}+\rho_{13}+L} c(\rho_{23})\, \mathrm{d}\rho_{23} \tag{10}$$

which comes out by averaging $c(\rho_{23})$ over all distances ρ_{23} that are compatible with given values of ρ_{12} and ρ_{13}. In Eq. (10) $m_1 = \max(|\rho_{12} - \rho_{13}| -$

Downloaded At: 08:51 28 January 2011

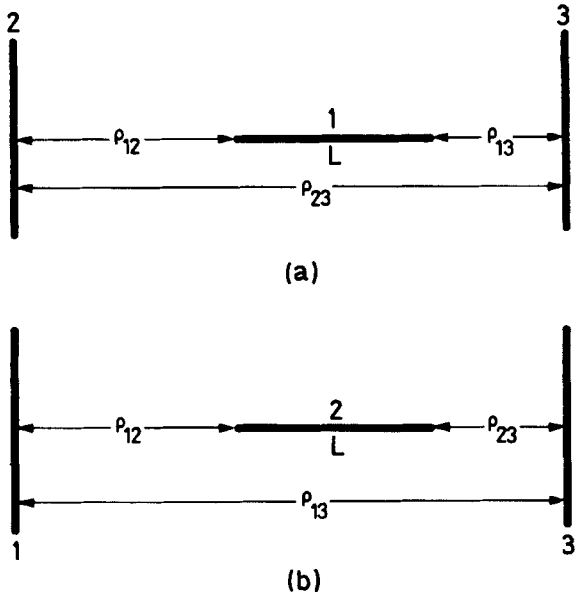

FIGURE 1 Illustration of the integration limits in Eq. (10). (a) upper limit; (b) lower limit.

Downloaded At: 08:51 28 January 2011

L, 0), and its integral limits are best visualized in Figure 1. The usefullness of $\langle c \rangle$, as defined by (10), rests on being only dependent on ρ_{12} and ρ_{13}, which facilitates integration of (9).

Taking the center of mass of particle 1 as the origin of coordinates, the geometry of convex bodies yields the well-known results[11]

$$\mathrm{d}\mathbf{q}_3 = \mathbf{u} \cdot \left(\frac{\partial \mathbf{R}_{13}}{\partial \theta} \times \frac{\partial \mathbf{R}_{13}}{\partial \phi} \right) \mathrm{d}\theta \, \mathrm{d}\phi \, \mathrm{d}\rho_{13} \, \mathrm{d}\mathbf{\Omega}_3 \tag{11}$$

$$\langle S_{c+\rho_{13}+c} \rangle = (8\pi^2)^{-1} \iiint \mathbf{u} \cdot \left(\frac{\partial \mathbf{R}_{13}}{\partial \theta} \times \frac{\partial \mathbf{R}_{13}}{\partial \phi} \right) \mathrm{d}\theta \, \mathrm{d}\phi \, \mathrm{d}\rho_{13} \tag{12}$$

where $\mathbf{R}_{13} = \mathbf{R}_3 - \mathbf{R}_1$: $\mathbf{u}(\theta, \phi)$ is the unit vector in the direction of the normal to the supporting plane of body 1 with respect to body 3 (Figure 2), and θ and ϕ are the polar angles of this vector direction.

Also for convex bodies

$$\langle S_{c+\rho+c} \rangle = 2S_c + 4\pi(2R_c^2 + 4R_c\rho + \rho^2) \tag{13}$$

which for a segment of length L becomes

$$\langle S_{c+\rho+c} \rangle = 4\pi\left(\frac{L^2}{8} + L\rho + \rho^2 \right) \tag{14}$$

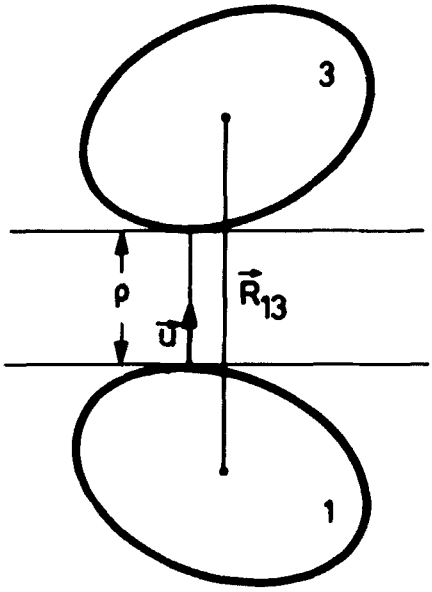

FIGURE 2 Geometry of the convex bodies 1 and 3; **u** is the unit vector normal to the supporting plane of body 1 with respect to body 3.

Downloaded At: 08:51 28 January 2011

The brackets $\langle\ \rangle$ mean average value with respect to the orientation of particle 3, of the indicated geometric functional for convex parallel bodies.

On the other hand, if $\rho_{13} < L$ molecules 2 and 3 may overlap for some of their mutual positions and orientations. When overlapping occurs, some forbidden configurations of molecules 1, 2 and 3, which should not contribute to Eq. (9), are artificially included through the integral in (10). As our last approximation we will assume that this contribution to $g(\rho)$ is negligible and then $\langle c \rangle$ may be computed by Eq. (10) inside the parallel body at the L distance.

The largest error in this approximation to the computation of function:

$$y(\rho) = g(\rho) \exp\left(\frac{u(\rho)}{kT}\right) \tag{15}$$

can be estimated by

$$\varepsilon\{y\} = \left| \int_0^L h(\rho_{13}) \langle c(\rho_{23}) \rangle \langle S_{c+\rho_{13}+c} \rangle \, \mathrm{d}\rho_{13} \right| \tag{16}$$

Computations about $\varepsilon(y)$ have shown that it does not appreciably affect computed values of $g(\rho)$, except at very high densities.

By using expressions (10)–(12) and (15) into Eq. (9) this one becomes

$$y(\rho) = 1 + n \int_0^\infty \langle S_{c+\rho_{13}+c} \rangle \langle c(\rho_{23}) \rangle h(\rho_{13})\, \mathrm{d}\rho_{13} \tag{17}$$

which in the Percus–Yevick approximation (8) takes the form

$$g(\rho) \exp\left(\frac{u(\rho)}{kT}\right) = 1 + 4\pi n \int_0^\infty \int_{m1}^{\rho+\rho'+L} (L^2 + L\rho' + (\rho')^2)$$
$$\times (\rho + \rho' + L - m_1)^{-1}(g(\rho') - 1))g(\rho'')\left\{\exp\left(\frac{u(\rho'')}{kT}\right) - 1\right\} \mathrm{d}\rho''\mathrm{d}\rho' \tag{18}$$

Equation (18), and the more Eq. (17), is a second order integral equation, similar to that of PY. Its comparative simplicity makes Eq. (18) amenable to a treatment by standard numerical methods. Unfortunately, it is not an exact convolution equation and therefore cannot be Fourier transformed in a product.

Downloaded At: 08:51 28 January 2011

III NUMERICAL RESULTS FOR THE PAIR DISTRIBUTION FUNCTION

Integral Eq. (18) has been solved for carbon dioxide and nitrogen. A linear segment was used as hard core and Kihara potential parameters are given in Table I.

Broyles method[9] was applied to solve the integral equation in the following way. For both fixed temperature and density, we try first as initial solution the corresponding to zero density or a density close to the given one if it is known from the previous calculations. An improved solution is then sought by an iterative procedure. Successive proposed solutions are a linear combination of the input and output functions of the preceding iteration cycle:

$$g_{\mathrm{IN}}^{(n+1)} = \alpha g_{\mathrm{IN}}^{(n)} + (1 - \alpha) g_{\mathrm{OUT}}^{(n)} \tag{19}$$

where n is the iteration cycle number and $0 < \alpha < 1$. A typical value for α is 0.9 about. As in the original Broyles' method, we have found that when an

TABLE I

Kihara's potential parameters used in this work. (From Ref. 17)

Substance	Core length	ε/k	σ
CO_2	2.30	316	2.940
N_2	0.93	117	3.207

approximate solution close to the actual one is reached, the method provides an exponential convergence towards the final solution. To improve this convergence rate Broyles' procedure[9] for infinite cycles was used. The double integral in Eq. (18) was evaluated by the Korobov and Labbude's method[12] using 144 points to guarantee an integration accuracy better than 1 %. (Occasionally we have used 987 points). The integration upper limit was set at $3\sigma + 2L$ after checking that higher values do not appreciably alter the value of $g(\rho)$.

Systematic calculations have been carried out for CO_2 in the 230–400 K temperature range and 20–1074 $\mathrm{Kg \cdot m^{-3}}$ density range. (Critical temperature and density are 304.21 K and 466 $\mathrm{Kg \cdot m^{-3}}$, respectively). For N_2 the corresponding ranges were narrower but equally meaningful. Calculations have been carried out on an IBM 360/65 computer requiring about 3 minutes of CPU time for a point in $T - \rho$ space and 60 Kbytes of permanent memory.

In Table II some of the calculated values[13] for $g(\rho)$ of CO_2 at 280 K and 1021 $\mathrm{Kg \cdot m^{-3}}$ are given. These data correspond to a reduced temperature $T^* = 0.756$ and reduced density $n^* = 0.405$, where

$$T^* = \frac{kT}{\varepsilon} \tag{20}$$

$$n^* = nV_{c+\sigma/2} \tag{21}$$

TABLE II

Pair distribution function for CO_2 at 280 K and 1021 $\mathrm{Kg\ m^{-3}}$

ρ/Å	$g(\rho)$	ρ/Å	$g(\rho)$	ρ/Å	$g(\rho)$
2.6	0.000	6.0	1.025	9.4	1.032
2.8	0.124	6.2	1.010	9.6	1.030
3.0	1.563	6.4	0.988	9.8	1.027
3.2	2.940	6.6	0.967	10.0	1.022
3.4	2.999	6.8	0.949	10.2	1.016
3.6	2.568	7.0	0.962	10.4	1.011
3.8	2.138	7.2	0.972	10.6	1.007
4.0	1.827	7.4	0.963	10.8	1.005
4.2	1.601	7.6	0.952	11.0	1.004
4.4	1.440	7.8	0.999	11.2	1.004
4.6	1.323	8.0	1.016	11.4	1.004
4.8	1.233	8.2	1.022	11.6	1.003
5.0	1.164	8.4	1.024	11.8	1.001
5.2	1.112	8.6	1.020	12.0	1.000
5.4	1.069	8.8	1.013	12.2	1.001
5.6	1.031	9.0	1.016	12.4	1.002
5.8	1.004	9.2	1.031	12.6	1.002

Downloaded At: 08:51 28 January 2011

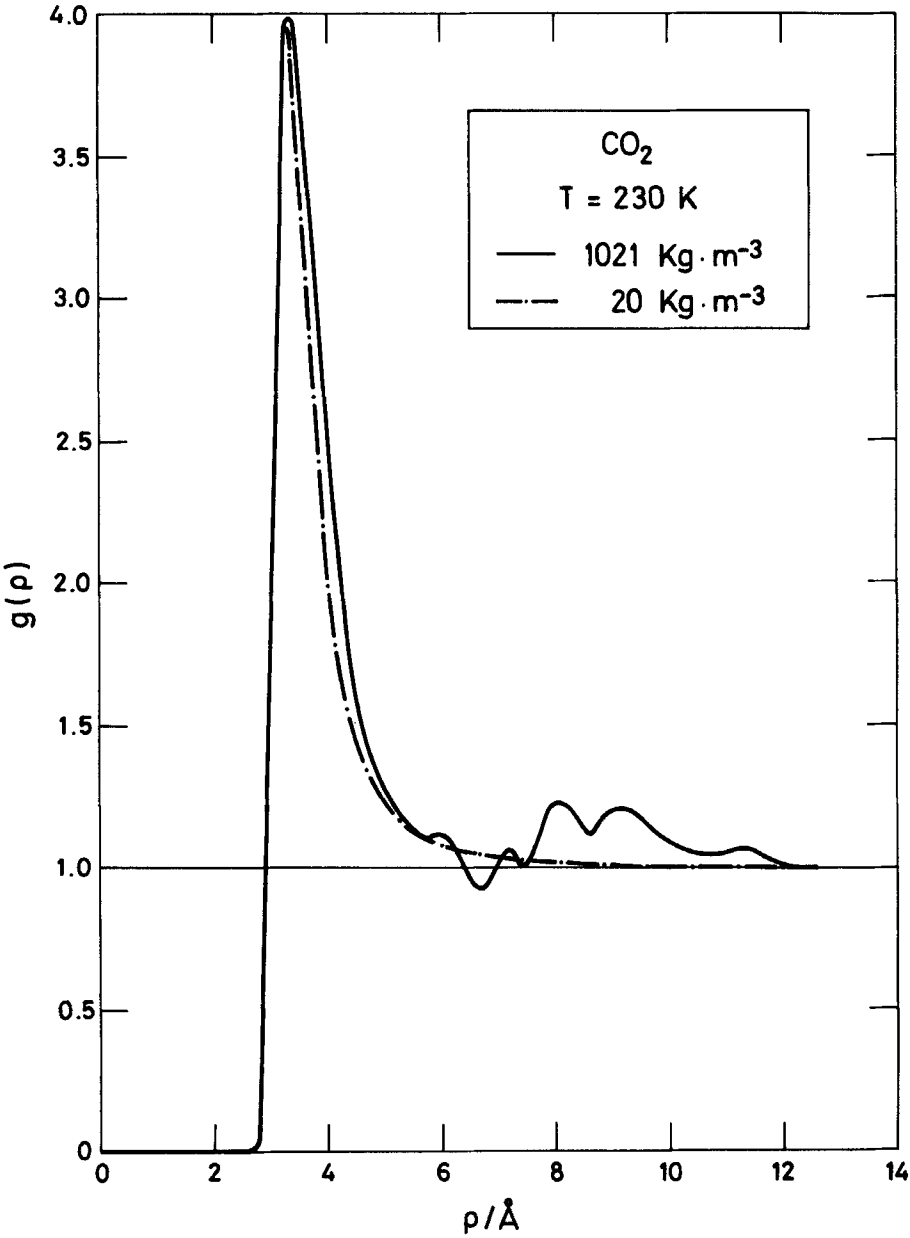

FIGURE 3 Pair distribution function of CO_2 at $T = 230$ K and two different densities.

Downloaded At: 08:51 28 January 2011

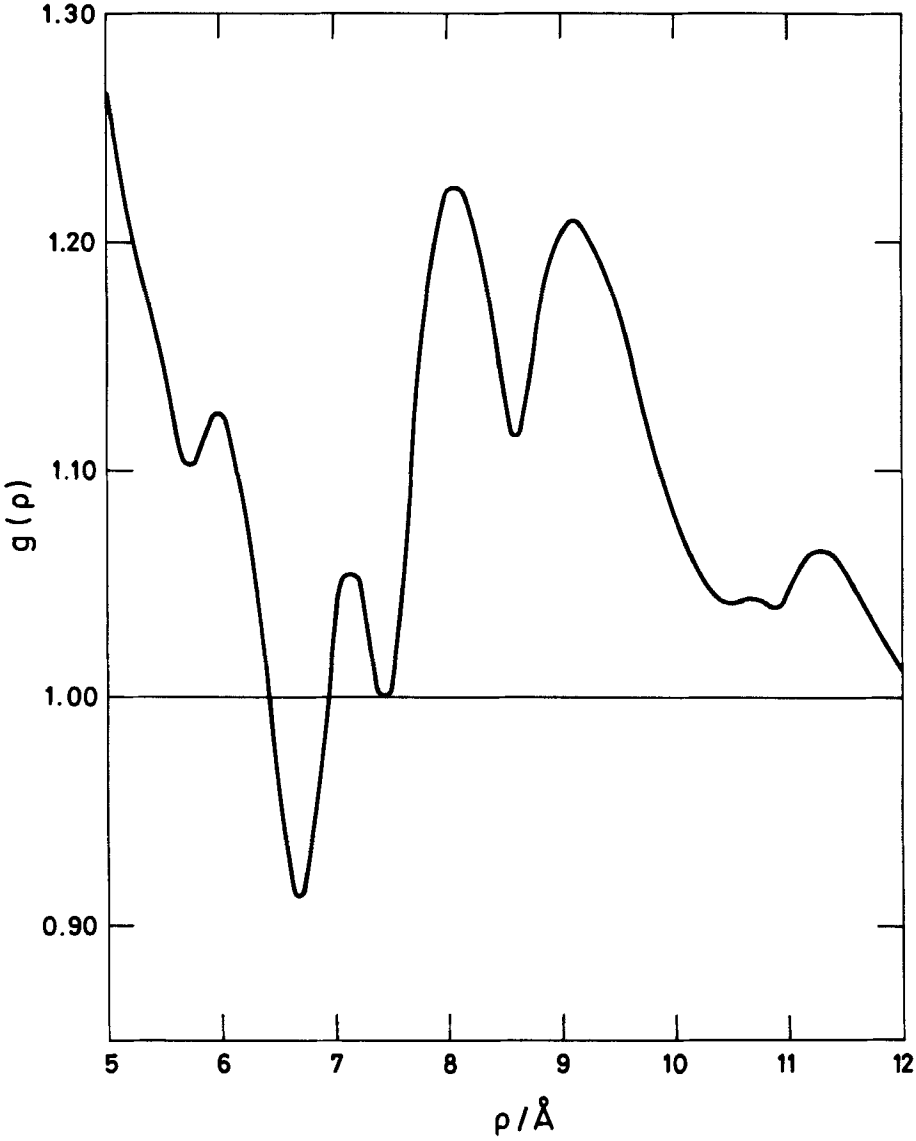

FIGURE 4 Detail showing the fine structure, in an expanded scale, of the distribution function of CO_2 plotted in Figure 3.

Downloaded At: 08:51 28 January 2011

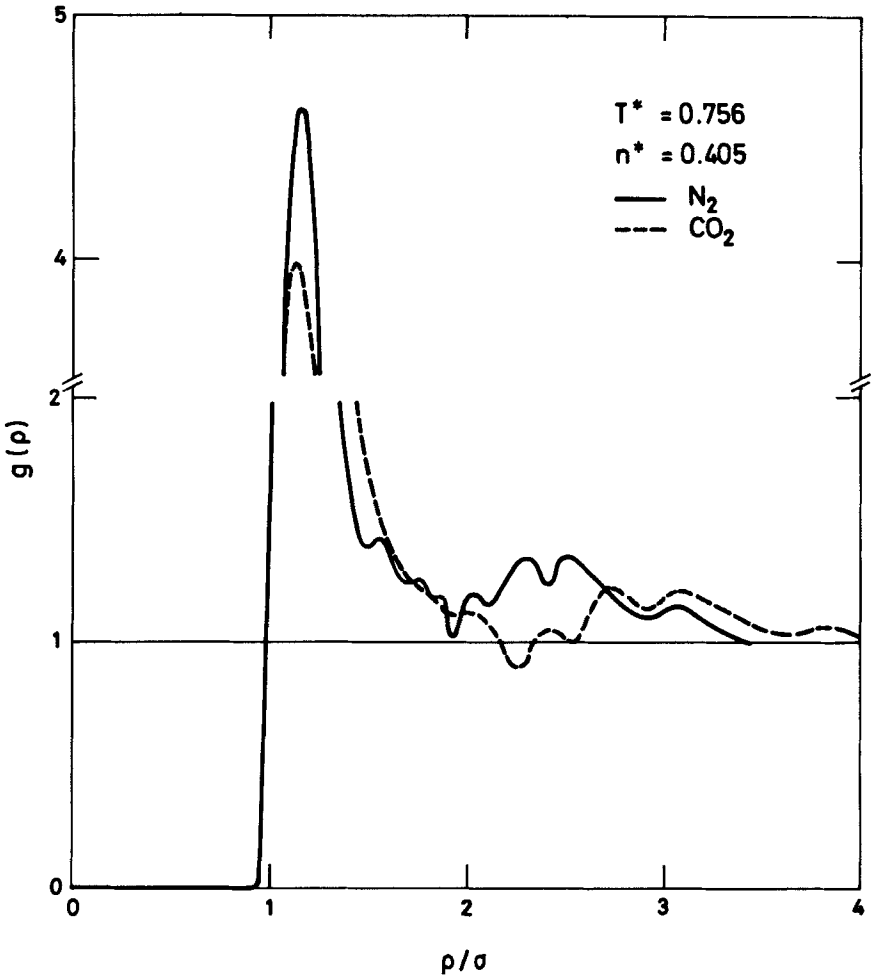

FIGURE 5 Pair distribution function of N_2 and CO_2 for $T^* = 0.756$ and $n^* = 0.405$.

The CO_2 pair distribution functions at low (20 $Kg \cdot m^{-3}$) and high (1021 $Kg \cdot m^{-3}$) density at 230 K, are plotted in Figure 3 against the shortest distance ρ. Features of the high density curve are shown in an enlarged view on Figure 4. Finally, Figure 5 allows comparison of CO_2 and N_2 distribution functions at the same reduced temperature ($T^* = 0.756$) and density ($n^* = 0.405$). As shown by Figures 3 to 5, the most striking feature of these results is probably the high degree of complexity displayed by the curve of the distribution function solution of Eq. (18). The almost periodic maxima and minima of the spherical molecules distribution function is replaced here by

Downloaded At: 08:51 28 January 2011

a larger and more complex set of maxima and minima. Consequently, up to a 3σ distance there are as many as 7 or 8 well-defined maxima. Undoubtedly such behaviour reflects a complex local structure to be expected in a fluid of non-spherical molecules, where to the position correlations, characterizing atomic fluids, other important correlations due to orientation are accrued.

IV TEMPERATURE AND DENSITY CHANGES OF $g(\rho)$

Although the linear core PDF behaviour with temperature shows a great similarity with that of PY's for spherical molecules,[13] is, however, more complex. Table III summarizes the maxima and minima values for N_2 and CO_2 at different temperatures and $n^* = 0.405$. As in the case of spherical potentials, it is noticed that a decrease in temperature makes more pronounced the maxima and minima, effect which is more noticeable when simultaneous changes in density occur. For instance, the first CO_2 maximum at $n^* = 0.202$ changes its value from 2.151 at 400 K to 2.688 at 300 K. Obviously, the first peak growth upon decreasing temperature should mean an increase in the number of nearest neighbours of the central molecule.

On the other hand, a decrease in temperature causes the distribution function structure to become more complicated. For instance, whereas the structure of the second and successive maxima is not very distinct at 400 K is more obvious at 230 K. The magnitude of changes with density seem to be dependent on temperature. They even change sign upon going from high to low temperature. For instance, we have found that the main CO_2 peak at 400 K increases from 2.16 to 2.23 when density goes from 60 to 1021 $Kg \cdot m^{-3}$, while at 310 K decreases first from 2.70 to 2.67 for n going from 20 to 400 $Kg \cdot m^{-3}$ and then increases up to 2.74 at 1021 $Kg \cdot m^{-3}$. Finally,

TABLE III

Heights of the successive maxima and minima in $g(\rho)$ for N_2 and CO_2 at $n^* = 0.405$ and several temperatures

	Nitrogen		Carbon dioxide			
T/K	85.1	100	230	280	310	400
1st max	4.740	3.278	3.986	3.086	2.814	2.280
2nd max	1.423	1.115	1.126	1.025	1.023	1.019
1st min	1.046	0.958	0.915	0.949	0.957	0.965
3rd max	1.347	1.141	1.224	1.012	1.008	1.024
4th max	1.341	1.158	1.209	—	1.022	1.033
2nd min	1.103	1.047	1.040	1.002	1.001	1.000
5th max	1.156	1.061	1.066	1.0043	1.0037	1.003
6th max	—	—	—	1.0018	1.0011	—

Downloaded At: 08:51 28 January 2011

at low temperatures it decreases steadily so that at 280 K it goes from 3.00 at 20 $Kg \cdot m^{-3}$ to 2.92 at 1000 $Kg \cdot m^{-3}$.

In any case, it is observed that changes in the first maximum height due to density are less important than those due to temperature. However, the PDF as a whole undergoes appreciable qualitative changes with density. Figure 3 illustrates this situation for CO_2 at 230 K. It is apparent that in going from low to high density the PDF changes until it adopts its characteristic structure with its main maxima and minima, each one in turn consisting of a fine structure of secondary maxima and minima.

Existence of this complex structure has been confirmed by applying computer programs dealing with 987 points for a double integral, in order to lower the error in $g(\rho)$ below 0.1 %. Besides, in some cases, we have used the solution obtained by a Broyles' extrapolation as a new input solution at the same temperature and density, and have repeated the procedure through four extrapolations. Besides, such a non-periodical behaviour have been observed in the Monte Carlo results by Nezbeda and Boublík for hard spherocylinders.[14]

Downloaded At: 08:51 28 January 2011

V COMMENTS ON MOLECULAR FLUIDS STRUCTURE

The molecular cores used in the calculations above have the same geometrical shape and values for the S_c and V_c parameters ($S_c = 0$, $V_c = 0$). Therefore comparison of the curves at the same reduced density and temperature gives the variation with the mean curvature or segment length. Figure 5 shows that even if we make $\rho^* = \rho/\sigma$ the curves do not overlap completely. A few differences are observed. The maxima are less pronounced in the case of the longest molecule, CO_2, as if their distribution were more uniform. Besides more peaks are observed for N_2, e.g. a maximum at $\rho^* = 1.57$. CO_2 minima and in particular the first one are more pronounced as if the most unfavourable molecular positions were become more so upon increasing core length. If on the basis of their shape we assume that the couple of close peaks centered around $\rho^* = 2.36$ for N_2 and $\rho^* = 2.92$ for CO_2 are homologous, we see that there is a phase shift of about 0.55 reduced units of one curve with respect to the other. This shift could probably be adscribed to the length difference between two cores. The structure found at larger reduced distances for CO_2 could be caused either by this fact or by the long-distance quadrupole interaction somewhat averaged in the potential parameters.

The shortest distance is a quantity hard to handle to derive the fluid molecular structure and it does not seem to be adequate to obtain directly a mental picture of the fluid structure from the PDF. We can check, however, if our results agree with some kind of structure already suggested. If we

TABLE IV
Distances between neighbouring molecules in CO_2 crystals and positions of peak in $g(\rho)$

Peak	Peak positions	Distances in CO_2-crystals
1	3.38	3.29
2	?	4.97
3	5.96	5.71
4	7.15	6.64
5	—	8.12
6	8.08	7.96
7	9.09	9.33
8	11.27	10.69

consider that a high density fluid structure should not differ greatly from a solid, though it is more loose, we may accept the crystal structure as a good starting point.

CO_2 crystallizes in a face centered cubic lattice.[3] The high quadrupole moment of this molecule makes this lattice to be formed of four other simple cubic lattices with their molecules pointing to different directions within each lattice. Table IV compares the distances between neighbouring molecules in a CO_2 crystal obtained from Kihara and Koba formulae,[16] and the positions of successive peaks in our $g(\rho)$. The agreement is good for peak 1 and also for those numbered 3 to 6. The undetected second one in $g(\rho)$ is probably hidden under the unusual width of the PDF's first peak (refer to Figures 3 and 4). The agreement is less satisfactory for the observed last maxima in the distribution function.

Below 35 K N_2 crystallyzes in a lattice similar to that of CO_2 something which could explain the similarity between both molecular PDF's. However, the N_2 molecule middle point does not fall on a face of the centered cubic lattice. The point that does it divides the N—N bond in about the 4/7 ratio.[3] As far as we know no calculations have been carried out to determine the shortest distances in this lattice. This kind of data could confirm or refute whether the slight differences between both PDF's correspond to the effect of the shifted point.

VI CONCLUSIONS

Starting from the Ornstein–Zernike relationship and the PY closure we have obtained a non-linear integral equation for linear molecules. The new equation is solvable in a reasonable computational time by classical methods for numerical solutions of integral equations.

Downloaded At: 08:51 28 January 2011

Unfortunately, Molecular Dynamics computations do not exist for molecules interacting with a Kihara potential, but the PDF we have obtained agrees very well with a probable model for liquid CO_2 and a reasonable model for N_2.

Lastly, computed PDF shows some of the features of Monte Carlo calculations for hard spherocylinders.

Acknowledgements

One of us (S.L.) gratefully acknowledges a P.F.B.I. grant through the "Instituto Rocasoloano," of the C.S.I.C., to carry out this work.

References

1. J. A. Barker and D. Henderson, *Rev. Mod. Phys.*, **48**, 587 (1976).
2. B. M. Ladanyi and D. Chandler, *J. Chem. Phys.*, **62**, 4308 (1975).
3. T. Kihara, *Advan. Chem. Phys.*, **5**, 147 (1963).
4. See, e.g., D. Chandler, *Ann. Rev. Phys. Chem.*, **29**, 441 (1978).
5. See, e.g., W. B. Street and D. J. Tildesley, *Faraday Discuss. Chem. Soc.*, **66**, 27 (1978), and references cited therein.
6. T. Boublik, *Mol. Phys.*, **32**, 1737 (1976).
7. Y.-D. Chen and W. A. Steele, *J. Chem. Phys.*, **54**, 703 (1971).
8. A. Ben-Naim, *J. Chem. Phys.*, **52**, 5531 (1970).
9. A. A. Broyles, *J. Chem. Phys.*, **33**, 456 (1960).
10. P. A. Egelstaff, C. G. Gray, and K. E. Gubbins, in *M TP Int. Rev. of Science, Phys. Chemistry*, Series 2, vol. 2, ed. by A. D. Buckingham, Butterworths, London (1975).
11. T. Boublik, *Mol. Phys.*, **27**, 1415 (1974).
12. R. A. Labbude, Ph.D., *Theoret. Chem. Inst.*, University of Wisconsin at Madison, Report WIS-TCI-414 (1973).
13. More extensive tables can be obtained from the authors.
14. I. Nezbeda and T. Boublík, *Czech. J. Phys.*, **B28**, 353 (1978).
15. L. L. Lee and H. M. Hulbert, *J. Chem. Phys.*, **58**, 44 (1973).
16. T. Kihara and S. Koba, *J. Phys. Soc. Japan*, **14**, 247 (1959).
17. T. Kihara and A. Koide, *Adv. Chem. Phys.*, **33**, 51 (1975).

Downloaded At: 08:51 28 January 2011